Middle East Journal of Applied Sciences
ISSN 2077-4613

Volume : 07 | Issue :01 | Jan.-Mar.| 2017
Pages: 178-188

Petrology and Radioactivity of South Gabal Um Anab Feldspar veins and Pegmatite Bodies, North Eastern Desert, Egypt

Osama M. Draz

Nuclear Materials Authority, P.O. Box 530, El-Maadi, Cairo, Egypt.

Received: 25 January 2017 / Accepted: 15 March 2017 / Publication date: 20 March 2017

ABSTRACT

The area under consideration consists of igneous rocks of Late Proterozoic age. The outcropping rocks are syanogranite and granodiorite. Feldspar veins varying in thickness and forms. Most of the, pegmatite bodies encountered in the syanogranite rock occur as plug-like bodies and veins of variable dimensions. These studied pegmatites are mainly of zone type. They are composed of intergrowth of smoky quartz and pink K-feldspar enclosing several clusters of mica pockets. The results of radioactive measurements reflect the high concentrations of eTh and eU in the studied pegmatite samples and low concentrations of eTh and eU in the studied feldspar veins samples. The concentrations of eU in feldspar veins ranges between 3 and 9 ppm with an average of 6.11 ppm, while in pegmatites range between 55 and 121 ppm with an average of 89.3 ppm. The concentrations of eTh in feldspar veins ranges between 7 and 31 ppm with an average of 19.78 ppm, while in pegmatites range between 111 and 299 ppm with an average of 234.2 ppm. The Ra (eU) content in pegmatites reach 88 ppm with an average of 64.9 ppm, while in feldspar veins reach 20 ppm with an average of 9.11 ppm. The distribution of radioelements is due to both magmatic origin and hydrothermal redistribution. The high level of radioactivity in the studied pegmatites are mainly due to the presence of samarskite, uranothorite, thorianite, zircon and fluorite. Most of the studied radioactive minerals commonly occur in the metamict state.

Key words: Igneous rocks, Proterozoic age, Gabal Um Anab Feldspar

Introduction

Several studies worldwide have revealed the presence of granite-pegmatite hosted rare-metal mineralization including Nb-Ta oxides and zircon. The study area represents a part of Central Eastern Desert of Egypt, north Qena-Safaga asphaltic road. It covers an area about 70 km^2 of crystalline basement rocks in addition to Phanerozoic sediments. It is bounded by latitudes $26^0\ 43^{/}\ 40^{//}$ and $26^0\ 48^{/}\ 30^{//}$ N and longitudes $33^0\ 34^{/}\ 12^{//}$ and $33^0\ 42^{/}\ 51^{//}$ E. The present study aims to throw light on the geology, petrography and radioactivity of some feldspar veins and pegmatite bodies, existing in south G. Um Anab area.

Geologic Setup

The area south G. Um Anab comprises exposures of igneous rocks of Late Proterozoic age. These rocks are traversed by wadis mostly filled with Quaternary alluvium sediments. The cropping rock types (Fig. 1) comprise granodiorite, syenogranites and Post granitic dikes.

The granodiorites are the most predominant rocks exposed in the area. The granodiorites are intruded by syenogranites with sharp contacts and are frequently dissected by many dikes of felsic and basaltic composition (Fig. 2a).

The syenogranites occur as remarkably uniform in composition. These granites are represented in the mapped area by G. Ras Baroud as well as the southern portion of G. Um Anab. They occur as isolated pluton of circular to semicircular outline.

These rocks are characterized by their red and pink color high jointing (Fig. 2b). They are characterized by their resistance to weathering and hence they form the highest peaks in the study area.

Corresponding Author: Osama M. Draz, Nuclear Materials Authority, Cairo, Egypt P.O.Box530, El-Maadi, Cairo, Egypt. E-mail:draz_o_m@yahoo.com

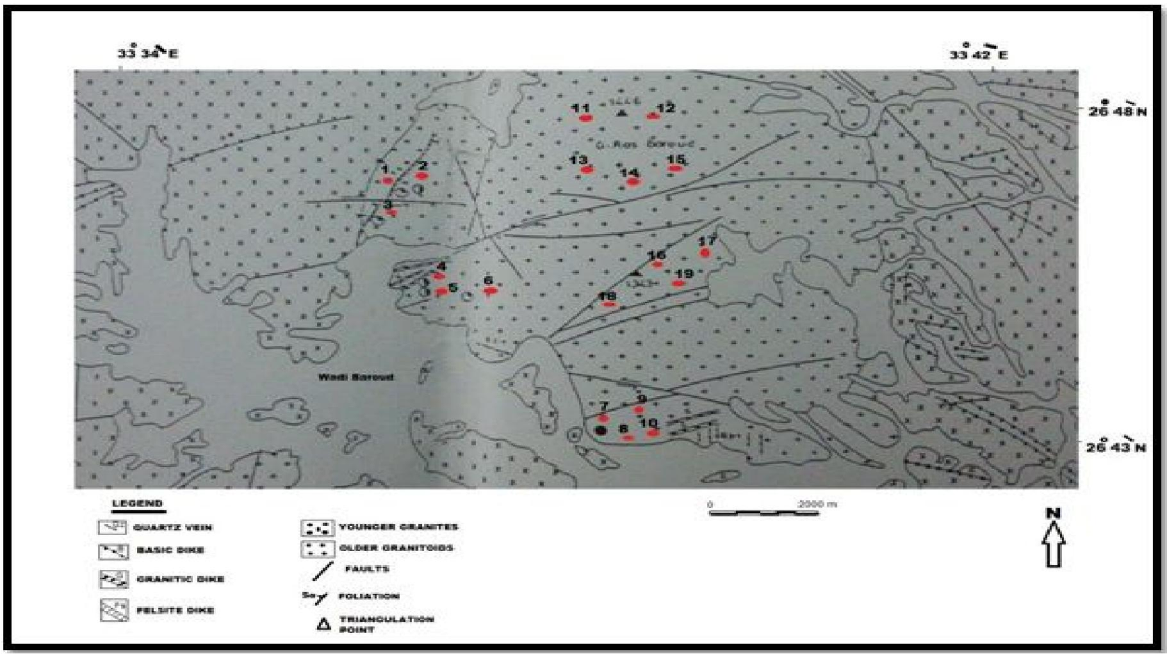

Fig. 1: Geologic map of the area after Omar, 1995.

Exfoliation, onion-skin texture and bouldery shape appearance are present, the weathering surfaces are characterized by a number of rounded to subrounded cavities of varying diameters (Figs. 2c & 2d). These cavities are named "Tuffoni weathering" Raguin (1965).

Numerous dikes and veins of different types and composition are recorded invading all the rock types exposed in the study area. A total number of 88 dikes and veins with total lengths of 1211 km are recorded.

	
Fig. 2a: Post granitic dykes	**Fig. 2b:** Joints with different directions
	
Fig. 2c: Exfoliation, onion texture and bouldery shape	**Fig. 2d:** Jointing and tuffoni weathering

Pegmatites are common in the studied area. They are found as pockets (Figs. 3a & 3b & 3c), mainly in syenogranites. The pockets are of varying size ranging between 0.3 and 18 m in width and from 0.4 to 23 m in length. They are mainly composed of intergrowth of coarse grained milky quartz and reddish pink K-feldspar with or without mica. Some of them show characteristic zoning, where the inner quartz cores are surrounded by an outer feldspar zone enclosing several clusters of mica. All pegmatite pockets show various radioactivity levels higher than their enclosing rocks.

Feldspar veins (Figs. 3d & 3e & 3f), attain a generally uniform thickness. They commonly include many vugs, some of them are occasionally filled with some iron oxides, carbonates and clays.

Fig. 3a: Pegmatite zone

Fig. 3b: Pegmatite zone

Fig. 3c: Pegmatite

Fig. 3d: Feldspar veins

Fig. 3e: Feldspar veins

Fig. 3f: Feldspar veins

Sampling and Techniques

10 samples were collected from pegmatites (1-10) and 9 samples were collected from feldspar veins (11-19) encountered in granites for radiometric and mineralogical studies. These samples were subjected to combination processes through a laboratory jaw crusher and roll mill. Determination of radioactive elements eU ppm, eTh ppm, Ra ppm (eU) and K% elements were obtained using the multi-channel analyzer of ϒ-ray spectrometry. A proper weight (300-350 gm.) of crushed samples were placed in a standard size plastic containers sealed well and left for at least 30 days to accumulate free radon and to attain radioactive equilibrium.

The samples were sieved and subjected to heavy liquid separation using bromoform solution (sp. gr. 2.82 g/cm^3) and methylene iodide solution (di-iodomethane with sp.gr. = 3.31 g/cm^3 the obtained heavy fractions have magnetic susceptibility. The magnetite was removed by hand magnet. The free magnetite heavy minerals fraction was fractionated using the High Intensity Frantz Isodynamic Magnetic Separator (model L-1). These magnetic fraction were examined carefully by the binocular stereomicroscope X-Ray Diffraction (XRD) technique using Philips X-ray diffractometer (Model PW-1050/80) and Environmental Scanning Electron Microscope (ESEM) using Philips Model XL-30 supported by an energy dispersive X-ray unit (EDX).

Petrographic Characteristics of Pegmatites

Pegmatites consist mainly of mega crystals of potash feldspar, quartz, plagioclases in addition to biotite and muscovite. Potash feldspar occur as subhedral to euhedral coarse grained crystals represented as perthihic and antiperthite crystals forming graphic texture with quartz and plagioclase. Most of quartz crystals occur as mega crystals. Plagioclases range in composition from albite to oligoclase. They occur as subhedral to anhedral crystals, characterized by lamellar twinning and sometimes corroded with potash feldspar and quartz. Biotite flakes are characterized by strong pleochroism from yellowish brown to dark brown color. Muscovite flakes are commonly associated with quartz and potash feldspar. Uranothorite commonly enclosed and associated with opaques as an aggregate of minute crystals. Zircon is present essentially as metamict or randomly distributed as fine to very fine-grain euhedral crystals commonly associated with biotite and rarely in plagioclase and quartz. Allanite occurs as a coarse prismatic euhedral crystals, honey faint brown in color with interference colors. Allanite is characterized by its high relief, fractured and display optically perfect zonations. Opaques minerals display an enrichment of parallel long stick like shape and occasionally occur as grains. Some biotite crystals are partially altered to chlorite and iron oxides. (Figs. 4 a & b & c & d & e & f) show the different photomicrographs for different minerals in pegmatites and feldspar veins.

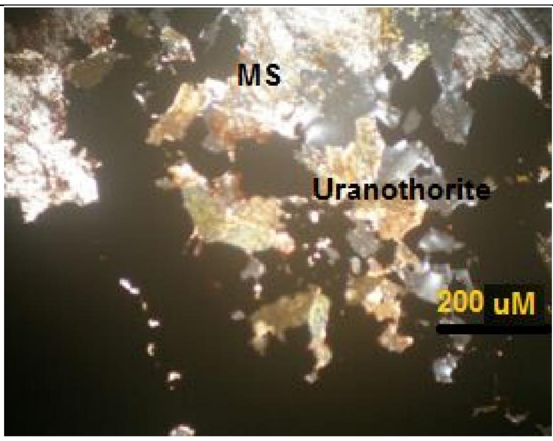

Fig. 4a: Uranothorite, zircon, muscovite crystals associated with opaques grains.

Fig. 4b: prismatic, honey faint brown allanite

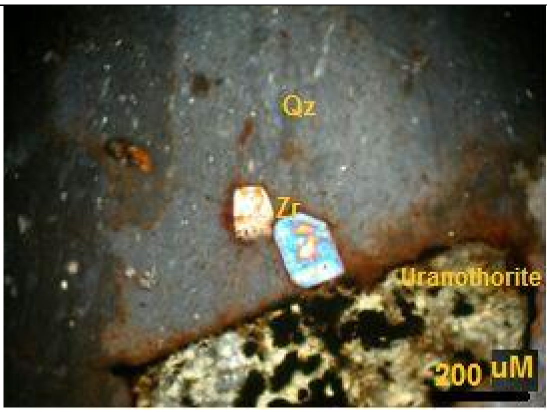

Fig. 4c: zircon, quartz with uranothorite and opaque.

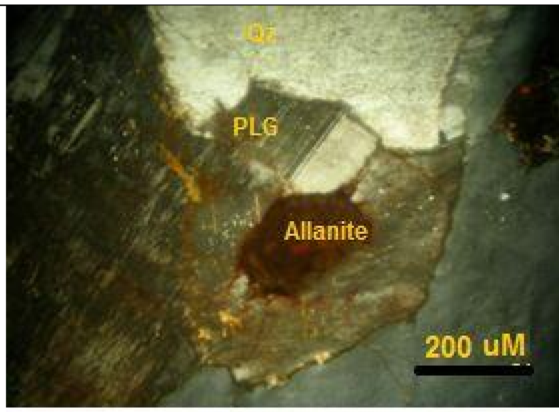

Fig. 4d: Allanite with biotite, quartz and plagioclase

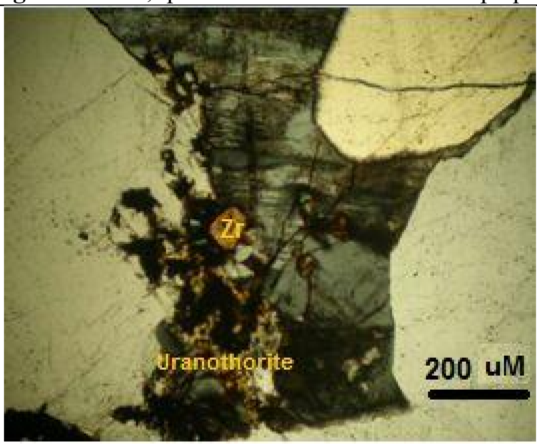

Fig. 4e: Uranothorite, zircon, muscovite crystals associated with opaques grains.

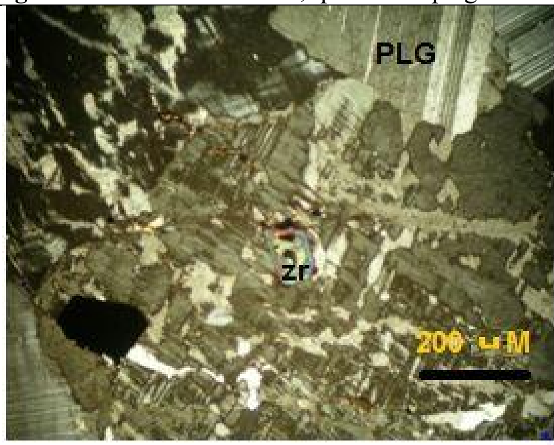

Fig. 4f: Zircon and plagioclase

Radioactivity

The results of radiometric measurements of eU, eTh, Ra (eU) and K for the studied pegmatite and feldspar veins samples with the calculated ratios eTh/eU are listed in table 1. The radiometric element concentrations of eU in pegmatites range between 55 and 121 ppm with an average of 89.3 ppm, while in feldspar veins range between 3 and 9 ppm with an average of 6.11 ppm, while eTh in pegmatites ranging between 111 and 299 ppm with an average of 234.2 ppm, while in feldspar veins range between 7 and 31 ppm with an average of 19.78 ppm. The Ra (eU) content in pegmatite reaches up to 88 ppm with an average of 64.9 ppm, while in feldspar veins reach up to 20 ppm with an average of 9.11 ppm. The results reflect higher concentrations of eTh and eU in the studied pegmatites than feldspars veins. Radiometrically, the studied pegmatites are considered as anomalous rocks, characterized by high content of U (>8 ppm) and/or Th (>16 ppm) (Dranely, 1982). Also, the results reflect low concentrations of eTh and eU in the studied feldspar veins, regarding to the studied pegmatites. The values of eU and eTh recorded in pegmatites are higher than those recorded for the world uraniferous pegmatite (av=28 and 21 for U and Th respectively, (Ford, 1982) as well as Egyptian uraniferous pegmatite's (av. = 33 and 28 ppm for U and Th respectively, Moharam, 2004 & 2006).
The average eTh/eU ratio of the pegmatites and feldspar veins are 2.64 and 3.14 respectively which means that these rocks are rich in uranium. Also, they are slightly less than the average continental crust value of approx. 3.8 (Van Schmus, 1995).

The eU – eTh variation diagrams for the studied pegmatite bodies and feldspar veins (Fig. 5a), reflect positive correlation indicating that the magmatic processes played an important role in the concentration of these radioelements. The eTh /eU and eTh variation diagrams for the studied pegmatite bodies and feldspar veins (Fig. 5b), shows that there are ill-defined relation, while there are negative relations between eTh /eU and eU (Fig. 5c), suggesting that the distribution of radioactive elements is due to the enrichment of eU according to eTh and magmatic processes as well as hydrothermal redistribution (Charbonneau, 1982).

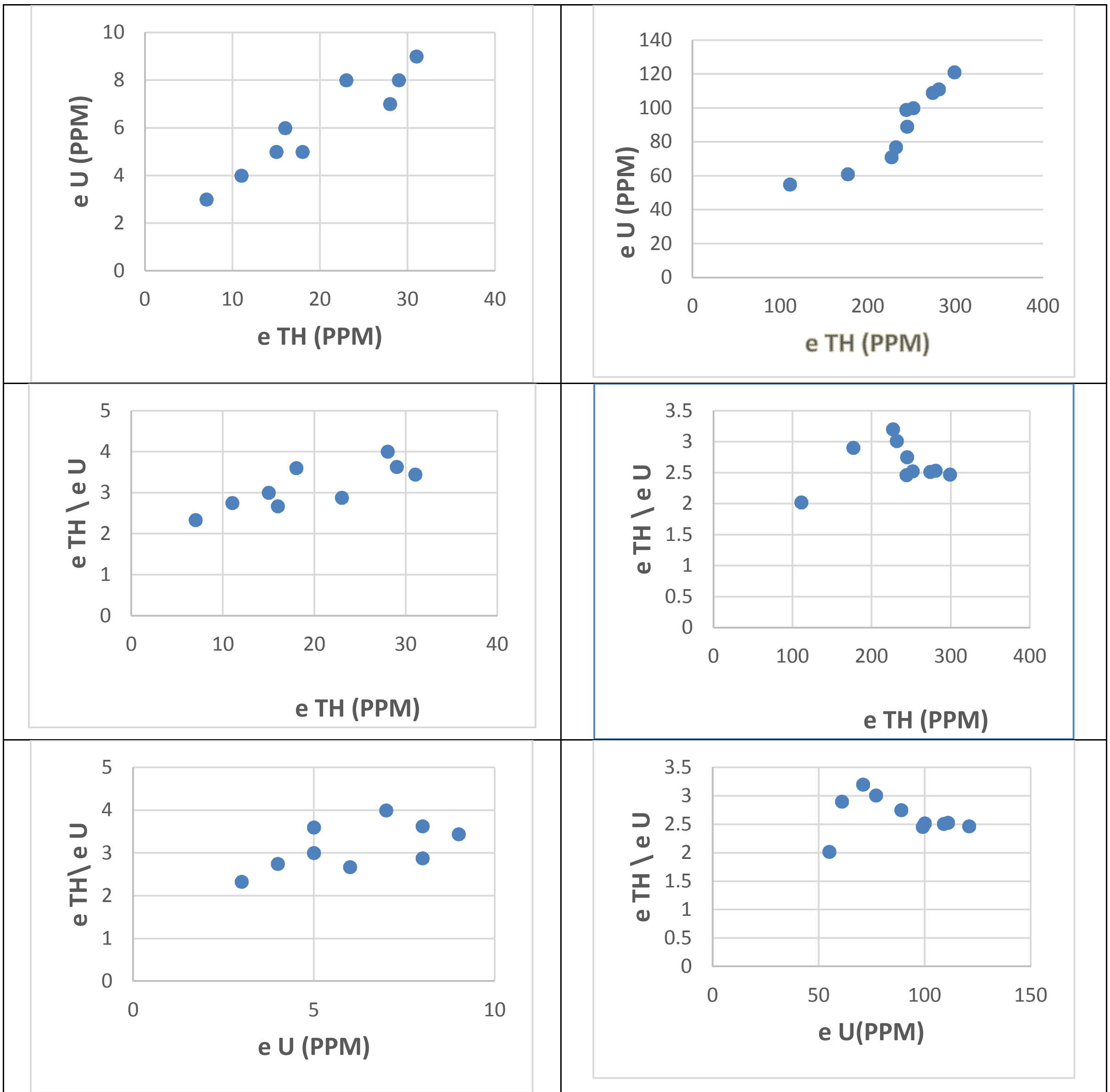

Feldspars veins	Pegmatite bodies

Fig. 5 : Binary relationship between a) eU versus eTh, b) eTh versus eTh/eU C) eU versus eTh/eU

Mineralogy of Some Pegmatite Bodies

The identified radioactive minerals separated from the heavy fractions of pegmatites are:- samarskite, uranothorite, monazite, zircon, columbite, fluorite and hematite are present.

Samarskite

Under binocular microscope, samarskite crystals are generally massive with a granular form. They are characterized by a splendid vitreous or resinous luster. They are mainly of velvet - reddish brown to bloody red in color. They are generally translucent, compact, metamict and hard. Samarskite is usually found in appreciable amounts and distributed in all size fractions with a tendency to increase with decreasing grain size. The ESEM as well as EDX of samarskite mineral grains are shown in (Fig. 6a).

Table 1: Radioelements concentrations of eU, eTh, Ra(eU) and K with some ratios for studied pegmatite samples and feldspar veins.

Sample No.	eU (ppm)	eTh (ppm)	Ra(eU) (ppm)	K (%)	eTh/eU	eU/Ra
1	77	232	52	0.69	3.01	1.48
2	55	111	39	0.98	2.02	1.41
3	121	299	88	ULD	2.47	1.38
4	109	274	80	ULD	2.51	1.36
5	89	245	60	0.88	2.75	1.48
6	61	177	45	ULD	2.90	1.36
7	111	281	80	ULD	2.53	1.39
8	100	252	76	0.68	2.52	1.32
9	71	227	56	ULD	3.20	1.27
10	99	244	73	0.77	2.46	1.36
Max.	121	299	88	0.98	3.20	1.48
Min.	55	111	39	0.77	2.02	1.27
Av.	89.3	234.2	64.9	------	2.64	1.38
11	7	28	9	0.23	4.00	0.78
12	9	31	20	0.33	3.44	0.45
13	6	16	5	ULD	2.67	1.20
14	3	7	5	ULD	2.33	0.60
15	5	18	4	ULD	3.60	1.25
16	5	15	6	ULD	3.00	0.83
17	8	29	14	0.25	3.63	0.57
18	8	23	13	0.22	2.88	0.62
19	4	11	6	ULD	2.75	0.67
Max.	9	31	20	0.33	4.00	1.25
Min.	3	7	4	0.22	2.33	0.45
Av.	6.11	19.78	9.11	-----	3.14	0.77

Samples 1-10 = Pegmatite   Samples 11-19 = Feldspar veins

Zircon $ZrSiO_4$

Occurs as different shapes and habits such as, short prism, long prism, outgrowth, overgrowth, parallel twining, and elbow-shape twining. Also, they are colorless or colored. Zircon grains are recorded at different magnetic fractions. Zircon contains many inclusions mainly iron oxides. Some of zircon crystals have inclusions uranium and/or thorium which raise the radioactivity level of zircon (Silver and Deutch, 1963; Steiger and Wasserburg, 1966).

The brown or dark red varieties of zircon grains are either metamict or highly stained with iron oxides. Metamict zircon has relatively high uranium and/or thorium content which cause damage for destruction of the zircon structure due to the dissipated energy during the decay of the radioactive element (Morgan and Auer, 1941; Hurely and Fairbairn, 1952). The concentration of U and Th in zircon are usually much lower, 5-4000 ppm U and 2-2000ppm Th. Some of the zircon mineral grains were analyzed by (SEM) with back scattered electron microscope images of zircon grains are shown in (Fig. 6b).

Fluorite CaF_2

Fluorite in the studied pegmatites exhibit wide range of colors ranging from pale blue to dark violet with vitreous and resinous luster (Fig. 6c). Al-len (1952) concluded that the coloration of fluorite can be attributed to the action REE during the differentiation of the magma, during the manganese or distortion in the crystal structure. EDX mineral analysis of the mineral reveals that it is composed essentially of Ca and F with the presence of trace amounts (<3.5%) of Si, Al, Mn and Fe.

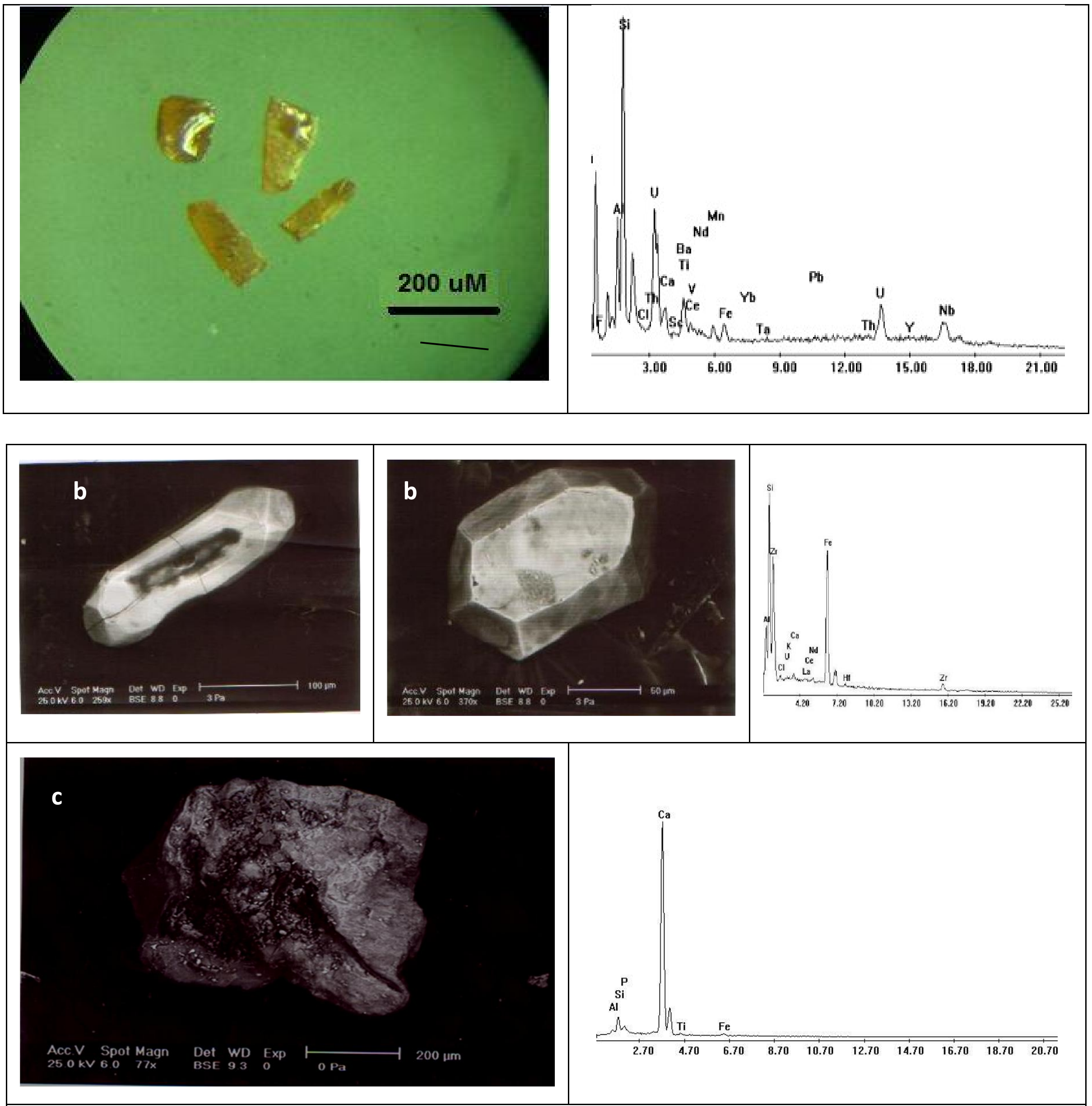

Fig. 6: a) Photomicrograph and XRD of samarskite b)Back scattered electron (BSE) image of zircon grains c) Back scattered electron (BSE) image of fluorite grains.

Uranothorite

Minute pale brown crystals are detected in the crushed powder of the pegmatites. SEM data are indicating the characteristic values of the radioactive mineral (Fig. 7a). U and Th represent the two main radioactive elements which their enrichment reflects its mineral name.

Monazite

It is one of the REE minerals and occurs in magmatic monazite (Normal) with normal Th and U contents. EDX data of hydrothermal monazite showed composition of P (17.93%), REE (59.55%), Th (1.59%), U (0.61%) with high Fe content (12.66%). XRD and EDX data of the magmatic monazite (monazite grown from a melt) show stichomythic composition of P (10.04%), REE (65.17%), Th (9.3%), U (4.3%) and relax of Fe (0.81%) (Fig. 7b).

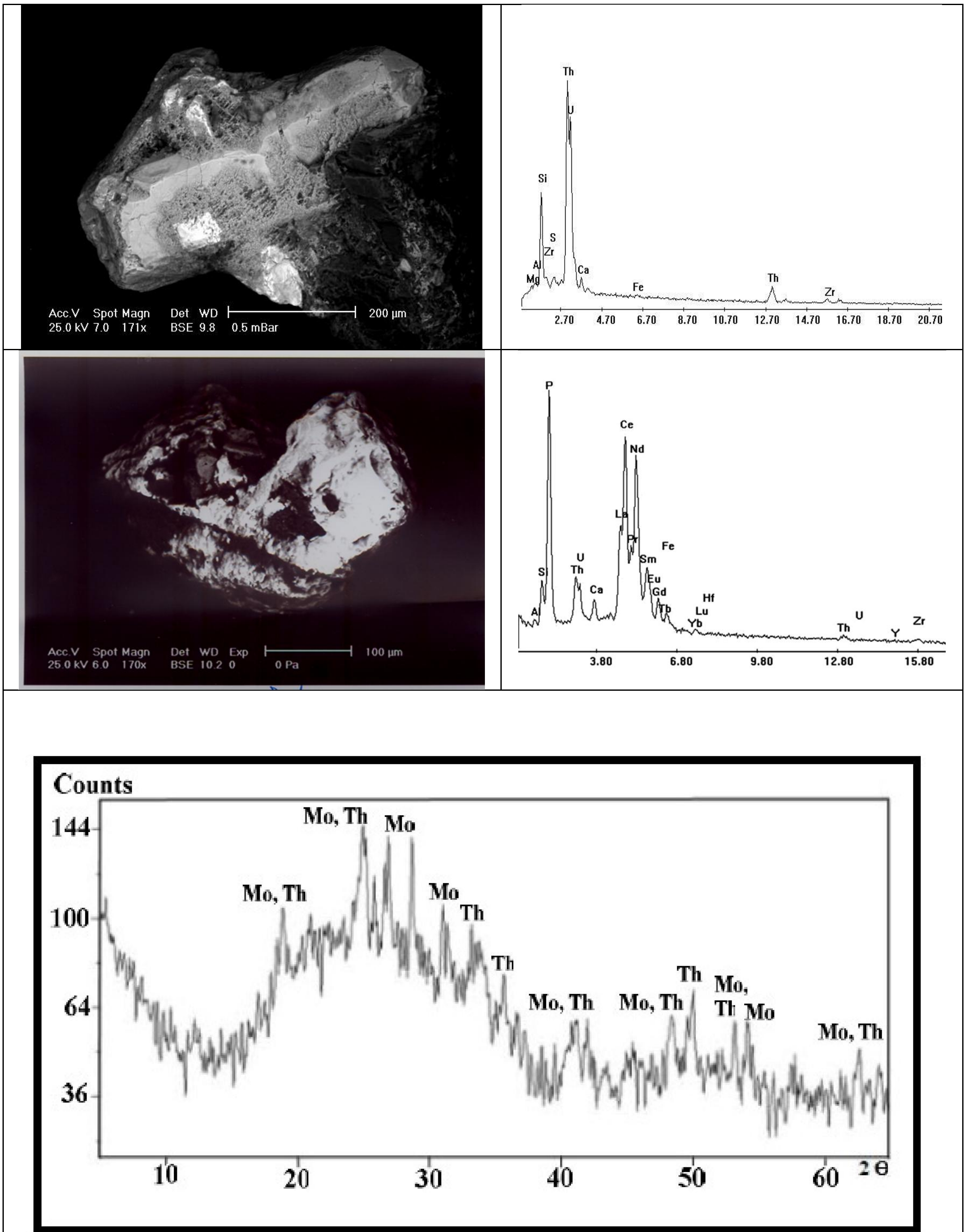

Fig. 7: a) Back scattered electron (BSE) image of uranothorite grains, b) Back scattered electron (BSE) image of monazite grains, c) XRD of monazite.

Columbite AB_2O_6

Members of the columbite-tantalite family of minerals also often contain significant U along with rare earths, Fe, Ca, and Th. The B site is either Nb or Ta. Like the pyrochlores, these minerals are associated with rare-earth pegmatites. Most of the compounds probably formed initially with U^{4+} most probably as a coupled substitution Ca^{2+} and U^{4+} for a trivalent ion. Oxidation occurs easily, however and most specimens contain significant amounts of U^{6+} (Smith, 1984).

Columbite minerals occur as black anhedral to subhedral crystals, in veinletes of 0.25mm to 0.5 in width. It is translucent and has a reddish brown color along the edges (Fig. 8a).

Hematite:

Occurs as cubic grains with reddish brown color. EDX composition show Fe (89.97%) with traces of S (0.81%), this neglected value of sulfur indicates that hematite formed after oxidation of pyrite (Fig. 8b).

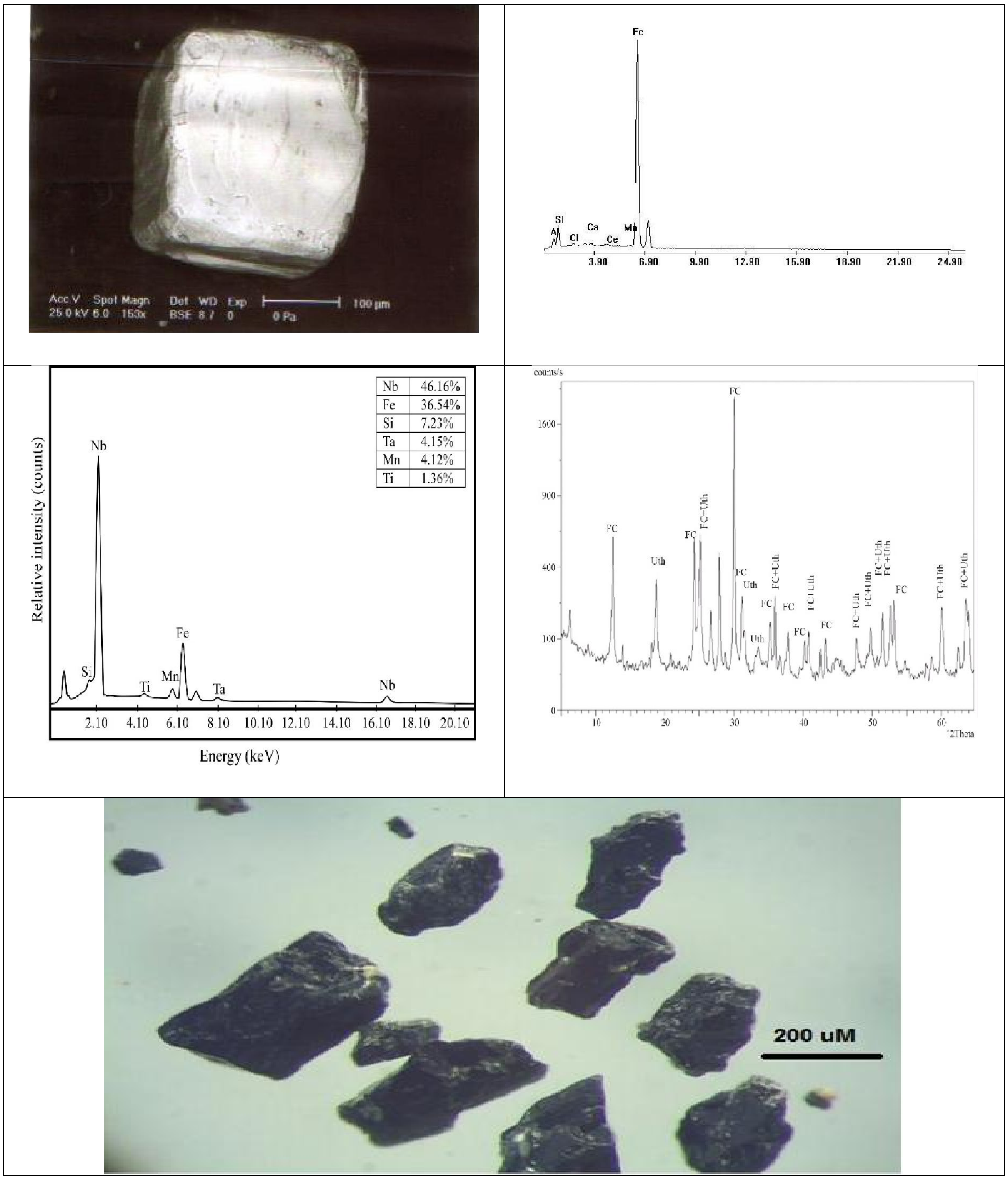

Fig. 8: a) Back scattered electron (BSE) image of hematite grains, b) Back scattered electron (BSE) image of columbite grains and XRD of columbite c) Photomicrograph of columbite

Conclusion

The rock types exposed in the studied area comprise granodiorites and syanogranites. The pegmatitic bodies and feldspar veins are hosted mainly in syanogranite. The pegmatite bodies occur as plug-like bodies of variable dimensions. The studied pegmatites are mainly of zoned type. The studied pegmatites can be considered as anomalies pegmatites being contain high contents of radioelements U and Th and formed in U-positive radioactive disequilibrium. The studied feldspar veins contain low values of radioelements U and Th. The distribution of radioelements can be attributed to the magmatic processes as well as hydrothermal alteration. The identified radioactive minerals in pegmatite bodies are Samarskite, uranothorite, monazite, zircon, columbite, fluorite and hematite.

References

Charbonneau, B. W., 1982. Radiometric granites in the Canadian Shield: Elliot Lake, Ontario; Fort Smith, Fury and Hecla, NWT. In: Maurice, Y.T.(Ed), Uranium in granites. Geol. Surv. Canada, 88-23, 91-99.

Ford, K.L., 1982. Uraniferous pegmatites of the Sharbot lake area, Ontario: In Maurice, Y.T. (Ed), Uranium in granites. Geol. Surv. Canada, 81-23, 125-138.

Hurely, M., Fairbairn, W., 1952. Age measurements from a part of the Brazilian shield. Bulletin 233-251.

Moharam, A. F., 2004. Uranium distribution in the Um Samra-Um Baraka granitic plutons and associated pegmatites, Central Eastern Desert, Egypt. Pro. 7yh Arab Conf. On the Peaceful Uses of Atomic Energy, II, 311-325.

Moharam, A. F., 2006. Petrology and Uranium distribution in the Um Samra-Um Baraka granitic plutons, Central Eastern Desert, Egypt. J. Fac. Educ., 31, 67-90. Omar, S. A. M., 1995. Geology and geochemical features of the radioactive occurrences of Om-Anab granitic masses, Eastern Desert, Egypt, M.Sc. Thesis, Cairo Univ., 174 p.

Morgan, E., C., 1941. Calculation of quietude, Ch. 1941.

Raguin, E. 1965. Geology of granite. Interscience Pupl. New York, 314p.

Silver, R. and Deutch, A. 1963. Polygenetic ophiolite belt of the California Sierra Nevada: Geochemical and tectonostragraphic development, p 223-235.

Smith, K. G. 1984. Standards for grading texture of erosional topography: Amer. J. Soc. Vol. 248, pp. 655-668.

Steiger and Wasserburg, 1966. Report about U, Th Pb dates for zircon at Proterozoic geology of the Southern Rocky Mountains.

Van Schmus, W, R., 1995. Natural radioactivity of the Crust and Mantle. In: Ahrens, T. J. (Ed). Global Earth Physics: A Handbook of Physical Constants. Am. Geophy. Union, AGU Reference Shelf 1, 283-291.